Optical Design of the WFIRST Phase-A Integral Field Channel

Guangjun Gao*[a], Bert A Pasquale*[b], Catherine T Marx[b], Victor J. Chambers[b]
[a] Sigma Space Inc. 4600 Forbes Blvd, Lanham-Seabrook, MD 20706
[b] NASA/Goddard Space Flight Center, Greenbelt, MD 20771
Guangjun.gao@sigmaspace.com, Bert.Pasquale@nasa.gov

ABSTRACT

WFIRST is one of NASA's Decadal Survey Missions and is currently in Phase-A development. The optical design of the WFIRST Integral Field Channel (IFC), one of three main optical channels of WFIRST, is presented, and the evolution of the IFC channel since Mission Concept Review (MCR, end of Pre-Phase A) is discussed. The IFC has two sub-channels: Supernova (IFC-S) and Galaxy (IFC-G) channels, with Fields of View of 3"x4.5" and 4.2"x9" respectively, and ~R 75 spectral analysis over waveband 0.42~2.0 μm. The Phase-A IFC optical design meets image quality requirements over the FOV areas while balancing cost and volume constraints.

Keywords: Space Instrumentation, Astronomical optics, Dark Energy, SN1a, Integral Field Spectography

1. INTRODUCTION [1~3]

WFIRST was selected as the top-ranked Astrophysics Decadal Survey Mission of the United States in 2010. It will provide fundamental and revolutionizing discoveries on dark energy and on the large-scale distribution of dark material. Dark energy is a repulsive force that is pushing the universe apart at an ever faster rate and dark material is most of the matter in the universe. WFIRST also investigates the demographics and properties of exoplanets, which are planets around other stars.

WFIRST includes two instruments, the Wide Field Instrument (WFI) and the Coronagraph Instrument (CGI). The WFI includes the Wide Field Channel (WFC) and IFC, both being designed and developed by Goddard Space Flight Center (GSFC). The WFC channel, which operates in the near-infrared (0.42-2.0 μm) range, has a field of view (FOV) 100 times that of Hubble. Its Focal Plane Assembly (FPA) has eighteen 4Kx4K detectors, and can output large-scale maps of the night sky at Hubble resolution. The Phase-A WFC channel has 6 filters for imaging mode and one GRISM for spectrographic mode. The second channel of the WFI is the IFC, which contains two image slicers (with different resolutions): IFC-S for supernova spectral imaging and IFC-G for galaxy redshift photometric calibration. Both IFC-S and IFC-G work in the wavelength range 0.42-2.0 microns, and share the same relay and spectrograph optics.

Three types of surveys will be executed with the WFI instrument: a High-Latitude Survey, a Supernova Survey, and a Bulge Microlensing Survey. The High-Latitude Survey will cover over 2,200 square degrees with imaging mode (4 NIR bands) and spectrographic mode (providing low-resolution spectral imaging). The Supernova Survey will have both imaging and IFC spectroscopy, the imaging survey is designed to find supernova, and the IFC spectrophotometric observations will be used to fully characterize the type and light curves of about 2,700 supernovae, chosen to sample the full redshift range. The Bulge Microlensing Survey will be mainly operated in the imaging mode of WFC, and can create highly-sampled light curves of about 56 million stars.

The block diagram of WFIRST in Figure 1 shows the relations of IFC to WFI and the whole WFIRST system as well.

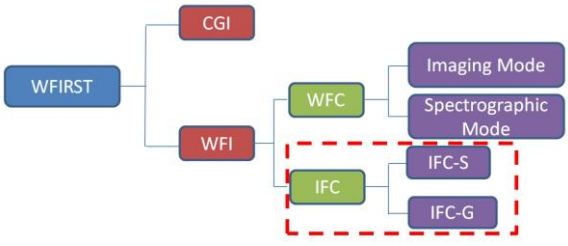

Figure 1. Block diagram of IFC in WFRST, the blocks circled by the red-dash line are the contents we will discussed in this paper.

A System-level description of IFC channel at the end of Phase-A, and the evolution of IFC ever since MCR are described in section 3. This is followed by details and results of IFC channel subsystem design in section 4. There is a brief report on the tolerance analysis and Monte-Carlo simulation of IFC optical system in section 5, and a summary of the Phase A IFC optical design in section 6.

2. OVERVIEW OF INTEGRAL FIELD CHANNEL [3]

There are four subsystems in the Phase-A IFC: Telescope and IFC relay, Receiving Optics, Image Slicers, and the Spectrograph. The telescope is shared by three channels: WFC, IFC and CGI, where WFC and IFC are two channels of the WFI (see Figure 1). Below the WFIRST primary mirror, three separate telescope FOVs are selected by three pick-off mirrors. These mirrors direct light to three groups of optics, one of which is the IFC relay optics. The other two are the CGI relay and the WFC imaging optics. The telescope and these three groups of optics form the Optical Telescope Assembly (OTA) (See Figure 2). IFC relay optics provide a collimated beam and a precise pupil position to the IFC Bench. The Receiving Optics focus the collimated beam from the IFC relay onto the mirror stack of image slicers at F/145.5. The Receiving Optics also provides mechanisms for on-orbit compensation of the defocus, image shift and/or pupil shift caused by the OTA's perturbations. There are two image slicers located at the image plane of receiving optics, IFC-S for supernova imaging and IFC-G for Galaxy imaging, with FOVs of 3"x4.5" and 4.2"x9" respectively. The image slicer assembly transfers the 2-D field images into a 1D "pseudo-slit" array. This array is the slit input of the spectrograph, which forms spectral image of the two slicers on the FPA. The layout of the IFC system is shown in Figure 3:

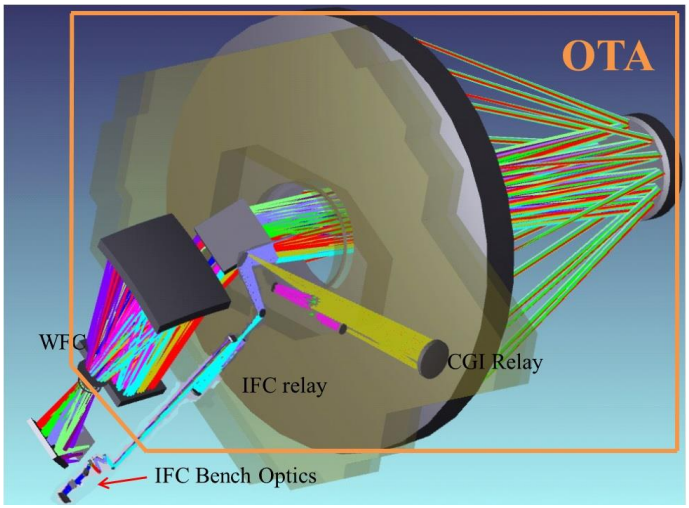

Figure 2. Layout of WFIRST OTA, IFC relay is included in OTA

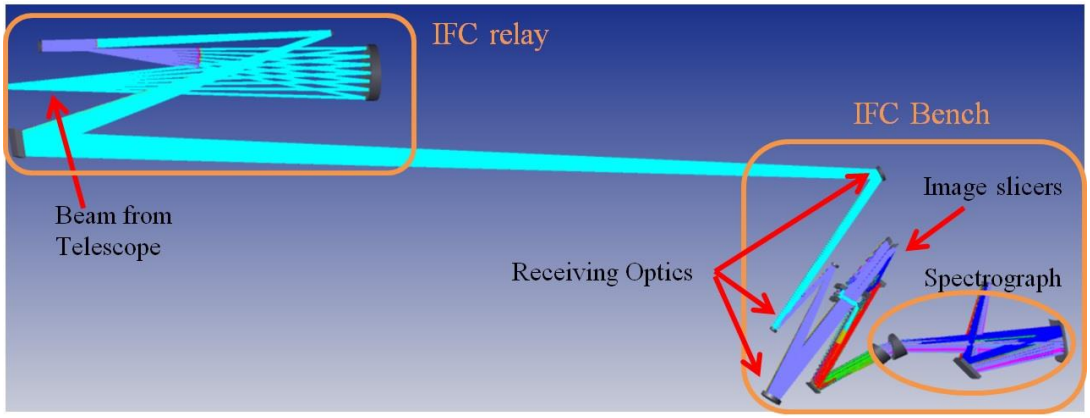

Figure 3. Layout of IFC system in Phase A, telescope is not included. Cold Pupil Mirror is the 2nd component of receiving optics.

3. CHANGES OF IFC SINCE MISSION CONCEPT REVIEW (MCR)

Since MCR at the beginning of 2016, there have been several creative changes introduced to WFIRST for the sake of reducing integration complexity and/or fabrication cost. In the IFC channel, the changes mainly include: moving the IFC relay to the OTA, inserting receiving optics before the image slicer, modifying parameters of the image slicers and rearranging the layout of the spectrograph. In this section, we will discuss the first three changes, and the last one can be easily understood by comparing Figure 3 (Phase A) and Figure 4 (MCR). The layouts of IFC channel (MCR version) is shown in Fig 4.

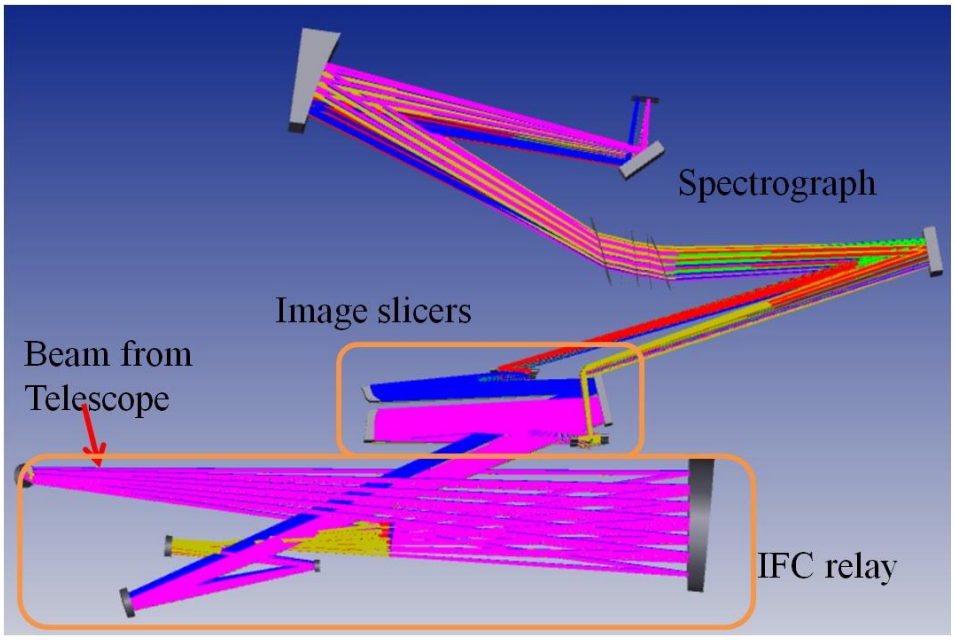

Figure 4. Layout of IFC system at MCR, for comparison to the layout of Phase-A version in Figure 3.

3.1 Merging IFC relay optics into telescope

The IFC relay optics are so named because they relay the intermediate image of the telescope to the image slicer. In the IFC MCR model, the IFC relay was considered as a subsystem of IFC instrument (see Figure 4), which lead to significant challenges for the testing and integration of the IFC bench and telescope because the image at the intermediate focal plane of telescope was seriously degraded by optical aberrations. The same issues existed in the integration of the WFC and CGI to the telescope. Therefore in Phase-A, the IFC relay is moved to the telescope as a subsystem of the OTA. The IFC relay balances the aberrations of telescope, outputs a collimated beam and projects the exit pupil of the telescope to the CPM (Cold Pupil Mirror) on the IFC Bench (as shown in Figure 3). With this architecture change, the interface between OTA and IFC Bench became greatly simplified.

An additional optical subsystem, the receiving optics, is needed prior to the image slicer to capture and focus the collimated beam from the OTA on the slice mirrors at F-number, F/145.5. Mechanisms (Tip/Tilt/Focus) are also included on some elements of receiving optics. Detail information of the optical design of receiving optics is covered in section 4.2.

3.2 Adjusting the parameters of the image slicer

In Phase A, we adjusted the parameters of image slicer (slicer width, aspect ratio, and number of slices) to reduce volume size and fabrication cost.

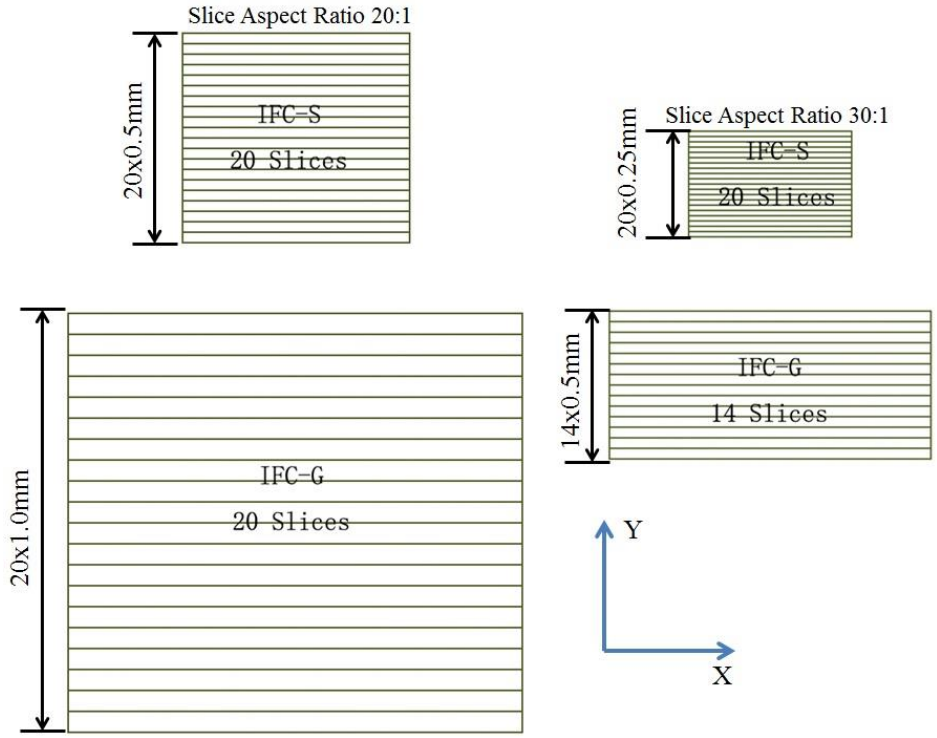

Figure 5. Layout of slicer mirror stack at MCR (a) and Phase A (b), the slice mirror size in the Y direction at MCR is 0.5mm for IFC-S, and 1.0mm for IFC-G; in Phase-A version, that size is 0.25mm for IFC-S, and 0.5mm for IFC-G.

Figure 5 shows the changes of the slicer mirror stacks from MCR to Phase-A. The first significant change is the size of the slices: in Phase A, slice widths for IFC-S shrink from 0.5mm to 0.25mm, and for IFC-G, 1.0mm to 0.5mm. This greatly reduces the volume of the slice mirror stacks while allowing the beam's F/# at the slicer mirror to decrease from F/291 (at MCR) to F/145.5 in Phase A. The second change is the number of slices in IFC-G being decreased from 20 (at MCR) down to 14 in Phase-A, allowing a reduction in cost. The loss of IFC-G FOV cause by reducing the number of slices is balanced by increasing the aspect ratio of the slice mirrors from 20:1 to 30:1. Therefore in Phase A, we have an image slicer with less fabrication cost, smaller volume and same or even larger FOV area covered. The detailed information of the image slicer (at MCR) and Phase A is summarized in Table 1.

Table 1. Comparisons of image slicer (MCR and Phase A)

	MCR		Phase A	
	IFC-S	IFC-G	IFC-S	IFC-G
Slice Width (mm)	0.5	1.0	0.25	0.5
Slice Quantity	20	20	20	14
Fov Area covered (arc sec sq.)	3x3	6x6	3x4.5	4.2x9
F-number at slice mirror	291	291	145.5	145.5
Magnification Ratio	5:1	10:1	4:1	8:1

4. OPTICAL DESIGN OF IFC SYSTEM

4.1 Optical Design of IFC relay

The WFIRST OTA includes the Optical Telescope, IFC relay, WFC aft optics and TCA of the CGI. The telescope's 2.4 meter aperture is shared by all instruments of WFIRST. The goals of the IFC relay optical design are to provide a collimated beam and image of the pupil to the CPM of the IFC bench.

The IFC relay has two fold mirrors and four powered mirrors. The two fold mirrors pick off and laterally translate the IFC beam alongside the WFC so that the optical path of these two channels are reasonably separated (see Figure 6 (a)). The powered mirrors R1-R4 balance the aberration of the telescope and output the collimated beam. In doing so, they also image the telescope's pupil on the CPM, located about 1.5m from the axis of the telescope. The layout of the IFC relay is shown in Figure 6.

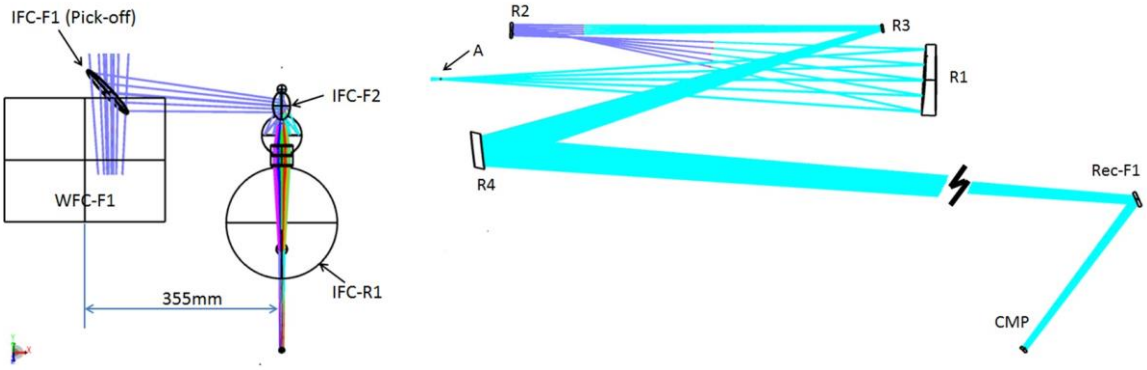

(a) (b)

Figure 6. Layout of IFC relay. (a) shows the 355mm distance between the WFC and the IFC channel, and (b) is the layout of IFC relay, R1, R2, R3 and R4. Position A is the intermediate focal plane of the telescope.

The RMS Wavefront Map of the IFC relay and the pupil image (using a paraxial lens at the position of CPM) are shown in Figure 7. The RMS wavefront value for the IFC-S ranges from 6nm to about 10nm, and the maximum RMS wavefront value of IFC-G is less than 16nm.

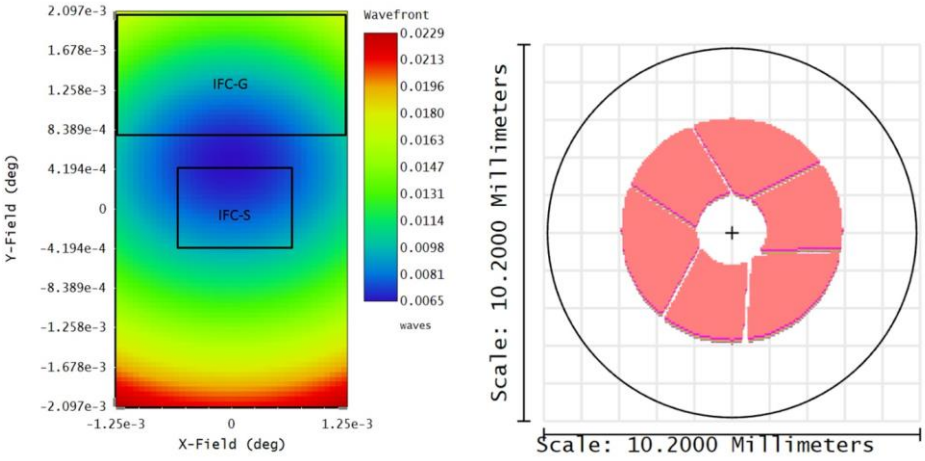

(a) (b)

Figure 7. Optical performance of IFC relay: (a) the RMS wavefront map evaluates at wavelength 1.0um, the two black frames are the FOV areas of IFC-S and IFC-G. (b) The pupil image of telescope on the CPM.

4.2 Receiving Optics

The receiving optics are the first subsystem located on the IFC Bench, between the IFC relay and Image Slicer. It focuses the collimated beams from the IFC relay to the slicer mirrors with F-number F/145.5. More importantly, it provides a telecentric image at the slicer mirrors, which can reduce the risk of vignetting occurring between slices of the image slicer. In addition, there are mechanisms in the mounts of the first fold mirror Rec-F1 and CPM to compensate the defocus and/or pupil shift caused by on-orbit perturbation of the OTA in the commission phase. In detail, the tip/tilt mechanisms on the Rec-F1 provide adjustment of pupil shift on the CPM, and tip/tilt/focus mechanism on the CPM provides adjustments of defocus and image shift on the slice mirror. The layout of receiving optics is shown in Figure 8.

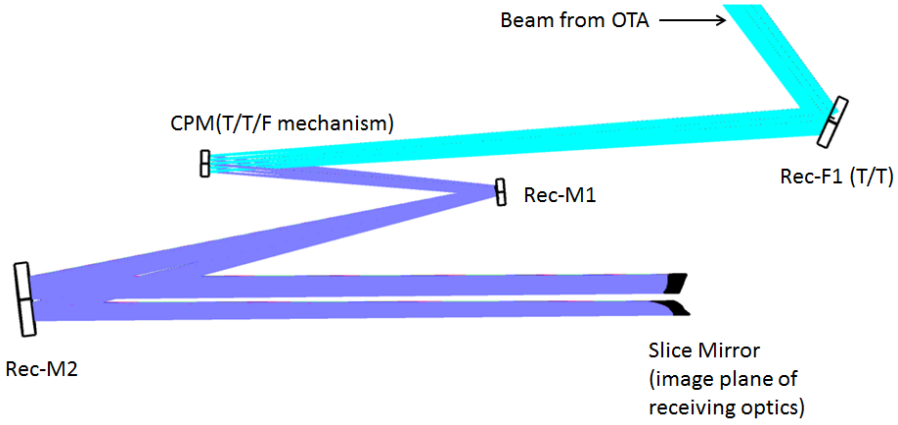

Figure 8. Layout of receiving optics

4.3 Image Slicer

The Image Slicer assembly, as the core subsystem of the IFC, "cuts" the 2-D image of receiving optics into slices, de-magnifies them, and re-aligns the images of these slices into single 1-D slit array, which becomes the input of the spectrograph. In WFIRST's IFC, there are two independent slicer stacks, one in IFC-S and the other in IFC-G. Figure 9 (a) is the schematic diagram showing the spatial mapping from 2-D image on the slice mirror block to the 1-D pseudo slits array of image slicers in IFC-S and IFC-G. The layout of the IFC image slicer is shown in Figure 9 (b). The magnification ratios of IFC-S and IFC-G image slicers are 4:1 and 8:1.

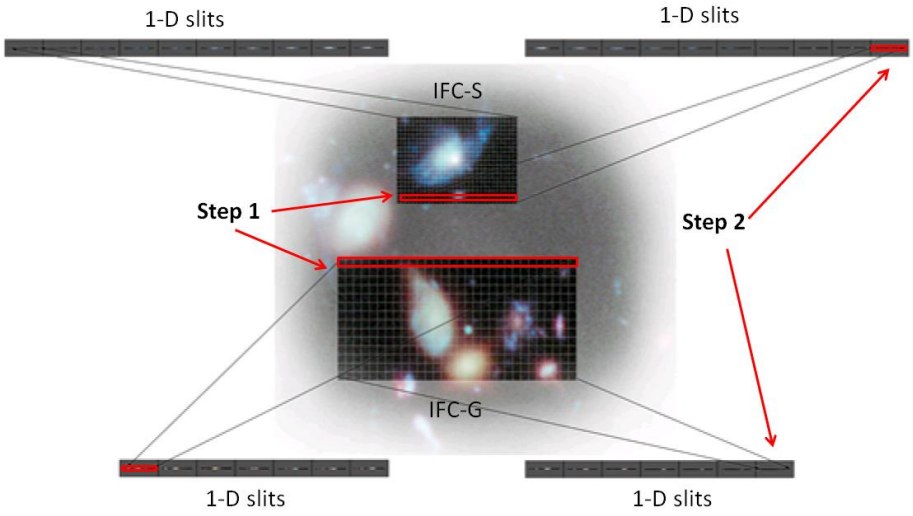

(a)

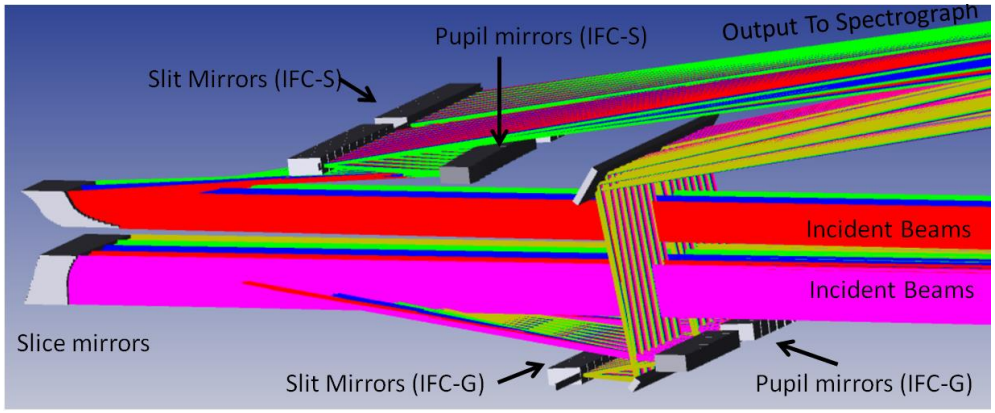

(b)

Figure 9. (a) spatial mapping relation from 2-D image on slice mirror stack to the 1-D pseudo slits array. The 2-D image is sliced by slice mirrors (step 1), and the slices are reimaged and realigned into 1-D slits as the inputs of spectrograph (step 2). In the WFIRST IFC, the process of reimaging and realigning is fulfilled by pupil mirror arrays. (b) is the layout of the image slicer in WFIRST.

One important feature in our image slicer design is the "hybrid" design of the slice mirrors. For an all-reflective type image slicer, the arrangement of slice mirrors is like a "C" curve shape in order to keep the constant magnification ratio in one image slicer given the distance between pupil mirror and pseudo slit is fixed. However, this "C" shape arrangement has a shortcoming of beam vignetting between neighboring slices, as shown in Figure 10 (a). To solve this issue, the upper half of the slice mirrors of IFC-S are aligned based on their right side, while the other half keep their original "C" shape design, as shown in Figure 10 (b). The same strategy is applied for the IFC-G slicer stack.

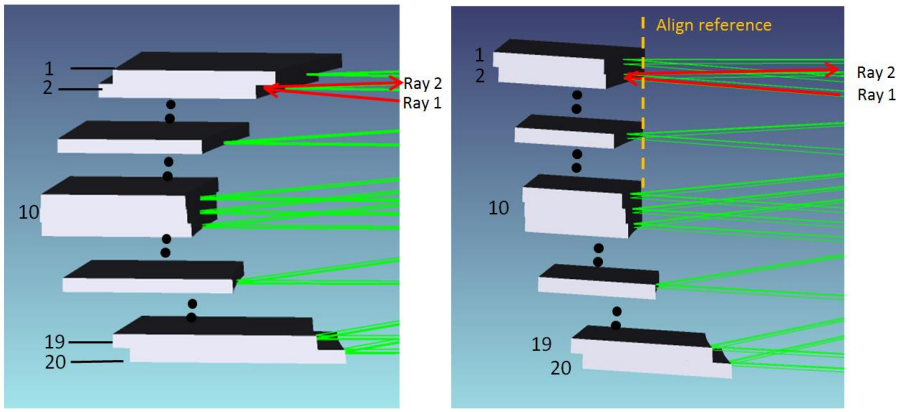

(a) (b)

Figure 10. Comparison of "C" shape (a) and "hybrid" (b) designs. In "C" shape design; the reflected beam (Ray 2 in plot) of slice #2 is vignetted by slice #1. In the "hybrid" design, there is no vignetting since the upper half slices are aligned along right side, the yellow dash line in plot (b).

4.4 Spectrograph

The spectrograph subsystem takes the signal of the pseudo-slit arrays as its input, and disperses the broadband signal perpendicular to the slit direction (see Figure 13 (b)), to form a 2-D spectral image on the FPA. In our spectrograph design, each individual pseudo-slit mirror has a radius of curvature to act as a field mirror. By adjusting the tip/tilts of these pseudo-slit mirrors, we can directly form a slicer exit pupil, where we locate the dispersion prism (see Figure 11(b)), creating a very compact layout. Although the beams passing through the prism are not collimated, they are very slow beams (about F/18 for IFC-G, and F/36 for IFC-S) and the small aberration caused by prisms can be balanced by the final aspherical mirror. The layout of the spectrograph is shown in Figure 11(a).

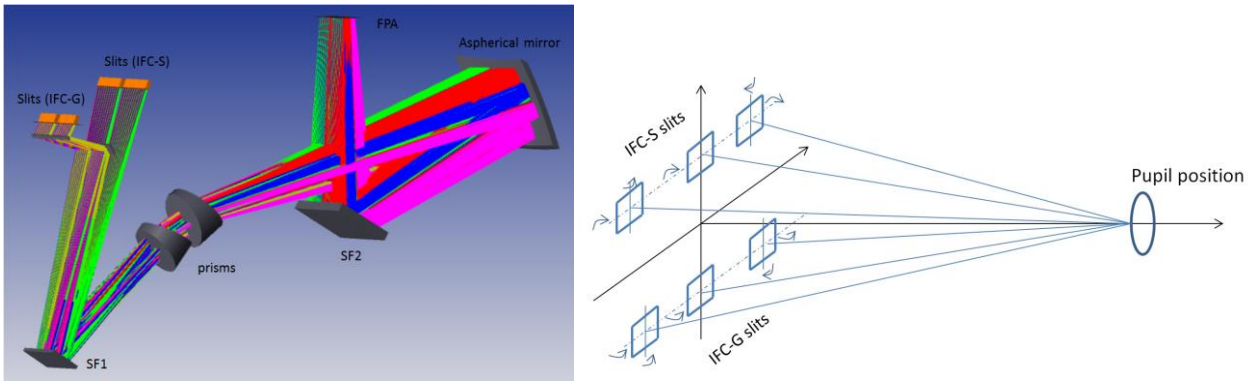

(a) (b)

Figure 11. (a) Layout of spectrograph. (b) The tip/tilts of pseudo slit mirrors adjusted to form a pupil image at the prism.

The dispersion elements are two identical prisms made of Fused Silica. Its dispersion curve on the FPA is provided in Figure 12.

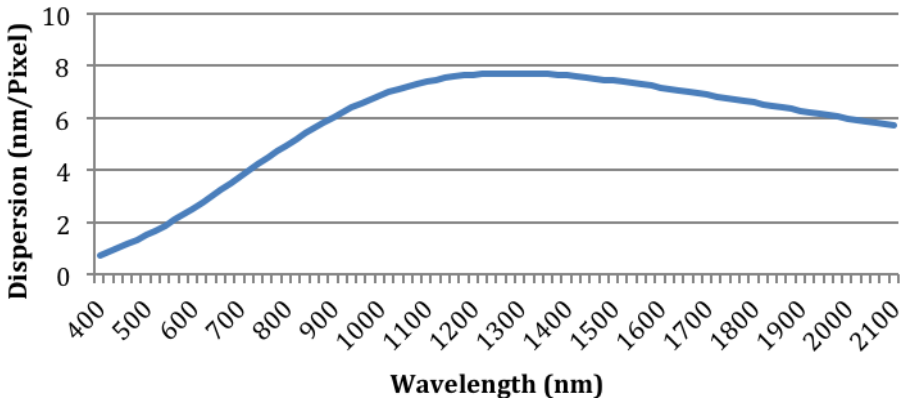

Figure 12. Dispersion curve of prisms on the FPA surface.

The maximum Wavefront error evaluated at the FPA is 41.9nm for IFC-S, and 61.2nm for IFC-G. The spot diagram of the 34 configurations (20 for IFC-S, and 14 for IFC-G) is shown in Figure 13 (a), and the footprints of all the configurations of IFC are shown in Figure 13 (b). Two sensors are used in the FPA, therefore the IFC can still output the full spectral signal of half the FOV areas if one sensor fails, which is referred to as "graceful degradation."

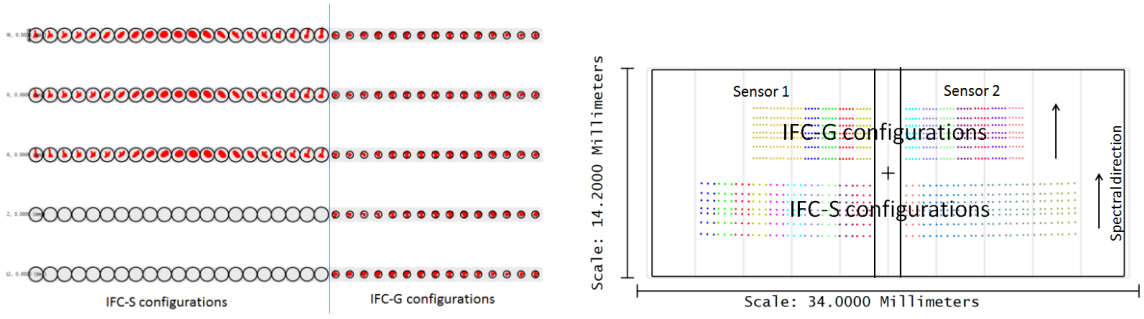

(a) (b)

Figure 13. (a) the spot diagrams of IFC channel, the left side is the spot diagrams of IFC-S, and the right side IFC-G. The wavelength is 1.0um. (b) The footprint of beams on the FPA plane.

5. TOLERANCES

We applied the fabrication and alignment tolerances on the nominal model and ran 100 Monte Carlo cases. For both IFC-S and IFC-G, we use the maximum RMS WFE as criteria to evaluate the performance. The cumulative probability curve is shown in Figure 14. It shows that 95% of IFC-S simulation samples have a maximum RMS WFE less than 92nm, and 138nm for the IFC-G.

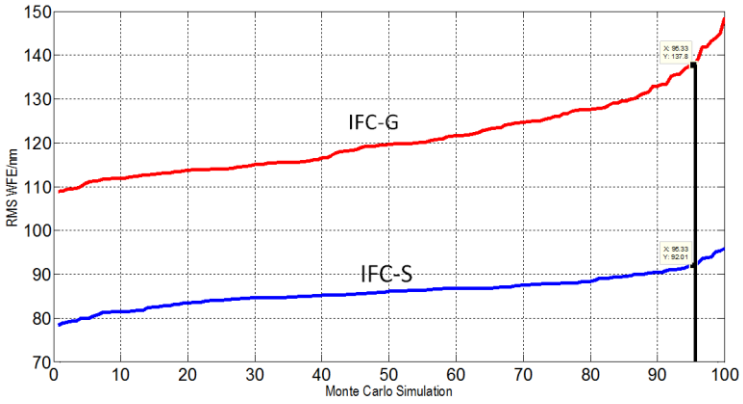

Figure 14. Cumulative probability curve of IFC Monte Carlo simulation

6. SUMMARY

We have briefly discussed the optical design of the sub-systems of the IFC channel in the Phase A of WFIRST. The major changes made to the IFC since MCR were discussed including the corresponding benefits over the old MCR version. The optical designs of each subsystem of IFC were reported. We evaluated the image quality on the FPA surface of nominal design and the 95% values of 100 Monte-Carlo simulations: the RMS WFEs of nominal design are 41.9nm (IFC-S) and 61.2nm (IFC-G), and the 95% values of Monte-Carlo simulations are 92nm (IFC-S) and 138nm (IFC-G).

ACKNOWLEDGEMENTS

This paper is based on the research and discussions conducted by the IFC engineering team and science team, we are grateful for the contributions of every team member. We appreciate the helpful support and suggestion provided by our colleagues: Yunhui Zheng from Sigma Space, Qian Gong, Nerses Armani and Patrick Williams etc. from NASA GSFC. This work was funded by the National Aeronautics and Space Administration (NASA).

REFERENCES

[1] https://wfirst.gsfc.nasa.gov/science.html
[2] Wide Field Infrared Survey Telescope (WFIRST) Starts Mission Formulation Phase, Roeland P, et al; STSCI Newsletter, issue 1 (2017)
[3] Optical Design of the WFIRST-AFTA Wide-Field Instrument, B. Pasquale, D. Content, et al; SPIE 9293 (2015)